Modifying and adjusting features of ZnO-based UV sensors through singly- and co-doping with Ti and Zr using low current sputtering technique

Nader Madani-Mashaei[1], Ebrahim Asl Soleimani[1,2]*, Hamidreza Shirvani-Mahdavi[1]

Abstract
The possibility of modifying and adjusting the properties of ZnO-based sensors in the post-fabrication stage is demonstrated by singly- and co-sputtering of ZnO thin films with zirconium and titanium nanoparticles. First, thin films of zinc oxide are created on glass substrates by sol-gel process and spin coating, and some of these films are converted to UV sensors through electrode placement on them by thermal evaporation method. Then, a number of the initial detectors are singly- and co-doped with Ti and Zr using sputtering deposition technique. Experiments show that the modification and adjustment of the parameters of the sensors through low current sputtering technique (LCST) is possible more efficiently and controllably. The transient response of all sensors are measured using I-t tests with periodic UV illumination before and after sputtering. Comparison of the results before and after doping shows that the photoresponsivity is improved on all doped sensors, and in many cases, a simultaneous improvement in this quantity and rise time is observed. In the best-case scenario, relative to undoped sensors, the photoresponsivity of the sensors doped with zirconium increases by more than 429 times, while the rise time of the sensors co-doped with titanium and zirconium decreases to less than 50%. This experience indicates that the modification and adjustment of the properties of ZnO-based sensors and actuators after electrode placement, to a large extent, is possible through LCST. It is noteworthy that this can be performed depending on the need and selectively in the shortest time, at the lowest cost.

Keywords
surface sputtering technique , transient response , photoresponsivity , rise time

[1] Department of Physics, Central Tehran Branch, Islamic Azad University, Tehran, I. R. Iran.
[2] Department of Electrical and Computer Engineering, University of Tehran, Tehran, I. R. Iran.
*Corresponding author: Ebr.Asl-Soleimani@iauctb.ac.ir

1. Introduction

In recent years, zinc oxide nanostructures, due to their environmental friendliness and some outstanding features such as wide bandgap (3.37 eV), high excitonic energy (60 m eV), and substantial piezoelectric constants, have been received significant attention and interests by sensor and actuator researchers and have found many applications [1–6]. Similar to other semiconductors, as many research works has been performed so far, the required properties of zinc oxide can be modified by the introduction of diverse dopants [7–10].

In conventional methods of manufacturing semiconductor sensors and actuators, dopants are often introduced into the pure semiconductor in the fabrication process, and then, the doped semiconductor is utilized to manufacture of them. As far as our studies indicate, so far no serious reports have been recorded on the modification and adjustment of the properties of detectors through doping after electrode placement. In the previous article, it was predicted that doping through sputtering can be used for manufactured sensors [11]. Therefore, in this study, it was decided to investigate the possibility of modifying and adjusting the properties of pre-fabricated UV sensors by doping method through sputtering.

So far, a large group of different dopants, including zirconium and titanium, have been used to modify the properties of zinc oxide for various sensor purposes [11–20]. In this research work, according to the experiences of the group, it was decided that the effect of the presence of nanoparticles of these two substances separately and also both together is examined on the performance of ZnO thin film based UV detectors by LCST. For this purpose, a number of UV detectors are first fabricated from sol-gel based zinc oxide nanofilms prepared by spin coating and electrode placement using thermal evaporation method in vacuum. Then, the transient response of the fabricated sensors is measured (I-t test). In the next step, these sensors are sputtered with zirconium, titanium, and both together at regular time intervals and then subjected to I-t test again. The results of these tests indicate that doping by LCST causes a significant change in the responsivity and response times of the fabricated sensors.

2. Methods

At first, several pure zinc oxide thin films were prepared by a double step sol–gel process exploiting spin-coating method, and then, the processes of electrode placement and doping were performed on the samples. Different tests and physical measurements were also carried out on the detectors whether before or after doping. The details of preparation and testing the samples are described as follows.

2.1 Sample preparation

Glass substrates were initially cleaned with acetone and deionized water, and then, for further cleaning and pre-preparation of the glass surface they were heated up to 550 °C in the ambient atmosphere for 1 h. Zinc acetate dihydrate, isopropanol, and diethanolamine (DEA) were used as the starting material, solvent, and stabilizer, respectively. The molar ratio of DEA to zinc acetate was maintained at 1, and the concentration of zinc acetate was selected equal to 0.5 M. Zinc acetate dihydrate was first dissolved in isopropanol, and the solution was stirred at room temperature at 500 rpm. After 1 h when the solution turned milky, while stirring the solution, DEA was added to it drop by drop such that a clear transparent homogeneous solution was yielded, and then, the resulting mixture was stirred at room temperature for another hour.

After aging for 24 h, the solution was deposited on the cleaned substrates by the spin coating method at room temperature, with a rate of 2000 rpm for 25 s. Having coated the samples, they were heated at 200 °C in the ambient atmosphere for 10 min to evaporate the solvent and remove the residual of organic materials. The coating and drying procedures were
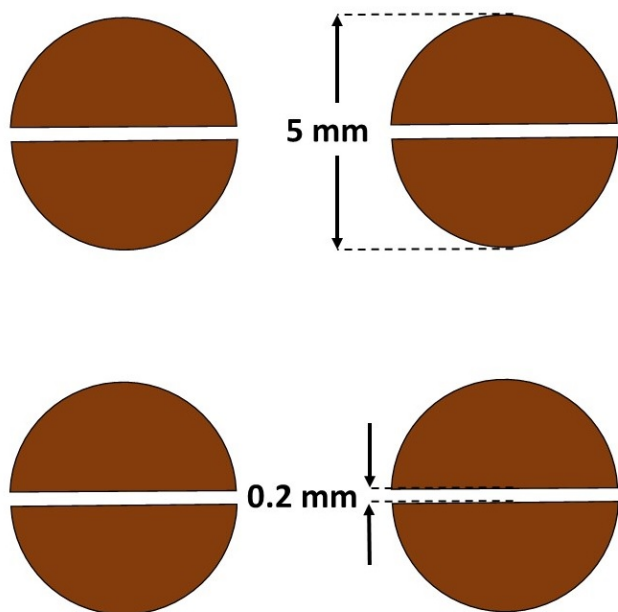
Figure 1. An example of a quad UV sensor module fabricated in this study, which includes four similar detectors on a substrate
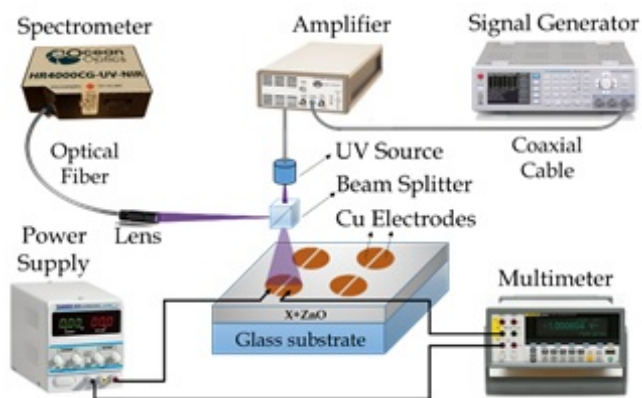
Figure 2. A schematic setup for I-t testing the fabricated UV sensors. The power of UV light source is measured by MAESTRO power meter with the low power thermopile XLP12 (from gentec-eo Co.) at the sensor predetermined location before placing the sensor in that location. The amplifier (model PZD 350A from Trek Co.) has been used to provide the power of UV source. The wavelength band of the beam splitter is in the range of UV light.

repeated two times to increase the film thickness. Finally, all the samples were annealed in ambient atmosphere at 550 °C temperature for 1 h.

To fabricate UV detectors, four circle-shape copper electrodes with the thickness 150 nm and a groove of 200 microns in the middle of each of them were concurrently produced through the thermal evaporation in vacuum on each of zinc oxide thin films Fig.(1). In total, nine such a sample, each including four electrodes, were fabricated.

2.2 Functional test of sensors

Prior to doping, all of the nine quad UV detectors were subjected to I-t test using periodic irradiation of 370 nm UV light with a periodicity of 60 s and a 4 V bias voltage. Figure 2 shows a schematic setup through which testing the fabricated sensors is performed. The LED type UV light source with the wavelength 370 nm and the full width at half maximum (FWHM) 30 nm generates an intensity equal to 0.5 mW/cm^2 on the sensor surface. The wavelength of the light source and its power in the sensor location were measured by the spectrometer HR4000 (from Ocean Optics Co.) and the MAESTRO power meter with the low power thermopile XLP12 (from gentec-eo Co.), respectively. The periodicity of LED light is adjusted by an accurate function generator HMF2550 (from Hameg Co.), and the current measurement is performed by a precision 6.5 digit multimeter 8846A (from Fluke Co.). To reduce the noise, the set-up was entirely placed in the metallic chamber connected with the earth.

After initial testing of all undoped detectors (pure samples) and recording of the results, to dope ZnO with titanium and zirconium, sputtering operation was performed. Three of the pure samples were doped with titanium (Group 1), three with zirconium (Group 2), and the remaining three with both
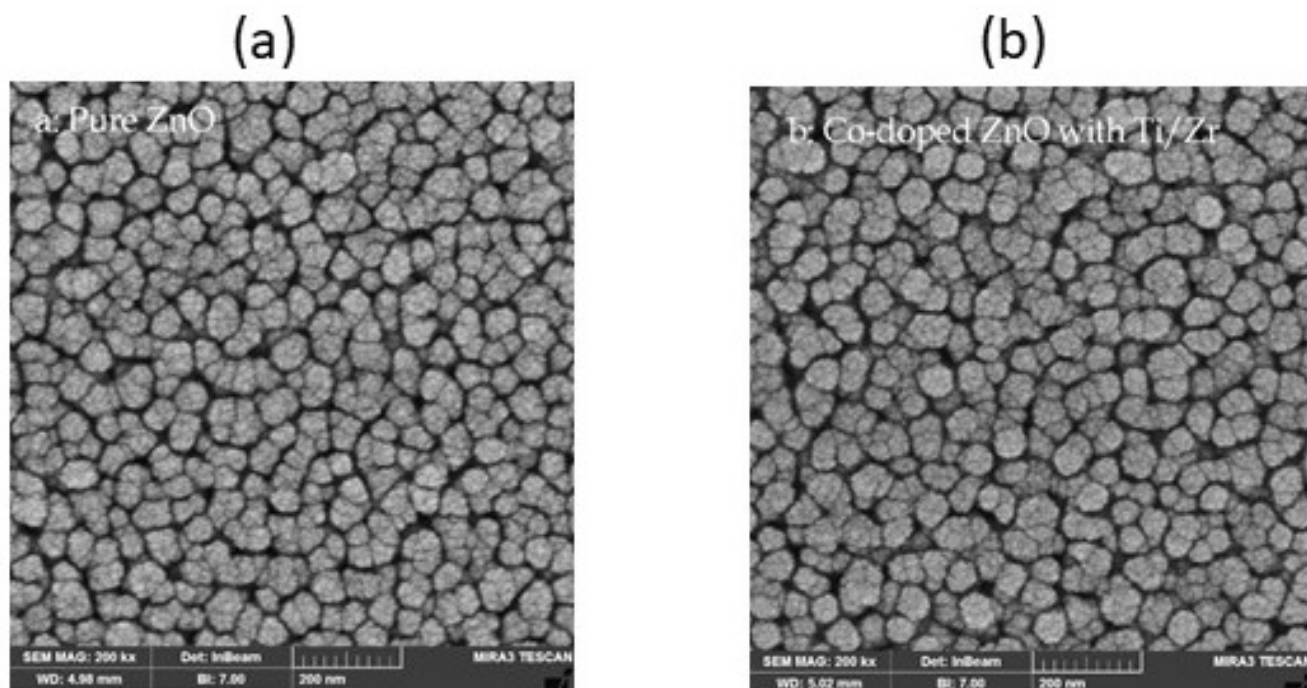
Figure 3. FE-SEM surface morphology images of a) the pure ZnO layer and b) the co-doped ZnO with Ti and Zr at 240 s sputtering for each of them.

(Group 3). The three samples of Group 1 were sputtered at different times of 120, 180 and 240 s, and the same process was performed for the three samples of Group 2. Whereas, the Group 3 samples were participated in both processes of groups 1 and 2, meaning that the three samples of Group 3 were separately doped once with titanium and once with zirconium each time at the different times mentioned above. Sputtering was performed for all samples under an argon atmosphere at a pressure of about 0.065 mbar and a current of 5 mA. After sputtering, the doped detectors were subjected to I-t test again with the same set-up and in the same conditions before doping. A number of pure and doped zinc oxide thin films were considered as references to study and compare their structural properties.

2.3 Characterization

X ray diffraction (XRD) analysis and Field effect scanning electron microscopy (FE-SEM) were utilized to study the crystalline structure and the morphology of doped and undoped samples, respectively. In addition, for optical analysis and evaluation of changes in light transmission due to the introduction of zirconium and titanium nanoparticles into pure ZnO films, the spectrum of all samples was measured by the spectrometer HR4000 (from Ocean Optics Co.). To determine the amount of zirconium and titanium and the ratio of their masses to ZnO mass, inductively coupled plasma mass spectroscopy (ICP- MS) was used. For this purpose, a number of doped films of each type were dissolved in HCl, and the resulting solution was exploited for the test.

3. Results and discussion

As mentioned, the detectors were first fabricated from ZnO thin layers and subjected to I-t test, and then, they were doped through LCST with zirconium, titanium, and both together and retested. The test results of each detector before and after doping were compared with each other. Since the doping of detectors is carried out after electrode placement, the impact of some effective parameters in the fabrication process of each detector is the same before and after doping. Consequently, it is expected that the difference in test results of the fabricated detectors before and after doping will be exclusively related to the doping effect of each detector.

3.1 Examination of surface features

To evaluate the effect of dopants on the morphology and size of the grains at the surface, FE-SEM image of the reference samples was captured before and after doping. Figures 3a and b respectively indicate images of the surface of a ZnO thin film before doping and after co-doping with Zr and Ti at 240 s sputtering for each of them. Here, the FE-SEM image of ZnO co-doped with Zr and Ti has been selected as a representative of all FE-SEM images. From these figures, one can find that the sequential co-sputtering of Zr and Ti has not had much effect on the morphology and dimensions of surface grains, implying that the dopants do not form a separate layer on the surface. Which this, of course, was predictable due to the very low current (5 mA) and relatively short sputtering time.
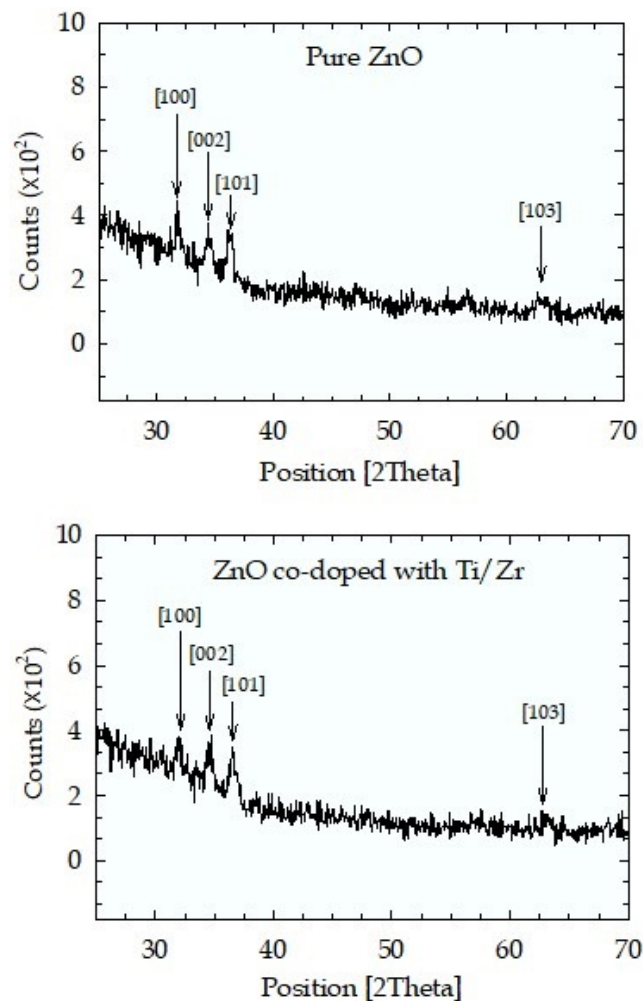
Figure 4. XRD spectra of the pure ZnO layer and ZnO co-doped with Ti and Zr through 240 s sputtering for each

3.2 Analysis of crystalline structure

To find out the crystal structure of thin films prepared and the possible effects of doping on them, X-ray diffraction was used to analyze these layers before and after doping. Figure (4) shows the XRD spectra of a pure ZnO thin film and a co-doped ZnO thin film with Zr and Ti through 240 s sputtering for each. The peaks of the plates, [100], [002], [103] [101] are obviously related to Wurtzite crystal structure of ZnO. The presence of multiple peaks indicates the polycrystalline nature of the layers. Comparison of the above spectra indicates that there is no significant difference in the intensity of the peaks related to the crystal plates, before and after doping. However, a slight increase in full width at half maximum (FWHM) of all three major peaks after 240 seconds of double sputtering could mean a slight increase in disorder of the crystal structure due to the introduction of dopants into thin films.

3.3 Optical properties

The transmission spectrum of all samples was taken in the range of 300 to 1000 nm. Figure (5) indicates the transmission spectra of ZnO thin films in terms of the sputtering time in the four following conditions: un-doped, singly-doped with Ti and Zr, and co-doped with Ti and Zr. As seen, all films have an average transmission coefficient of more than 83.6% in the visible range, and in many of them it even reaches more than 95%, which implies that this method of doping does not impact on the transmission coefficient much. Ti-doped films show the lowest reduction in transmission coefficients, so that their coefficients have decreased from 97% to about 95% on average, and this is while in other films the reduction of the coefficients is further observed. On the other hand, contrary to expectations, the lowest transmission coefficients are not related to the highest doping rate, but to 180 s of sputtering, which reduces the coefficient to about 83.6% for doping with zirconium and to about 83.8% for co-doping with zirconium and titanium. For the film that has been sputtered with zirconium for 180 s, a significant reduction in the transmission coefficient is also observed at wavelengths less than 370 nm. This means an increase in absorption in this range, and it could mean an improvement in the performance of detectors that have been doped to this extent with zirconium, a consequence that is also confirmed by I-t test. In the infrared region, a slight decrease in the transmission coefficient is observed in almost all films, indicating the formation of absorption levels with lower energy in this region in all doped detectors. Overall, it can be concluded from this discussion that dopants do not form a separate layer on the surface of the films, a subject that is also confirmed by FE-SEM images. Therefore, the cause of changes in the transmission coefficients of sputtered thin films should be further sought in changes in energy levels due to the formation of new bonds and defects in the surface of the films by dopant atoms.

3.4 ICP-MS test

In this study, by reason of the very high accuracy required and that the very small amount of material is utilized, the ICP-MS method with the precision of part per billion (ppb) was used to find out the mass ratio of titanium and zirconium to zinc in the films. For this purpose, five samples of ones with the longest double sputtering time were placed in 10 cc of high purity hydrochloric acid so that all the thickness of the co-doped ZnO layers with Ti and Zr was dissolved in acid, and eventually, the resulting solution was considered for ICP-MS test. The results show that the mass ratios of zirconium and titanium to zinc in films that were subjected to double sputtering with zirconium and titanium for 240 s and with a current of 5 mA are 0.096% and 0.023%, respectively. That the mass ratio of titanium to zinc is smaller than the mass ratio of zirconium to zinc can be for two reasons: more difficult sputtering conditions for titanium, and that, the atomic mass of titanium is significantly smaller than that of zirconium. It should be noted that although the amounts of titanium and zirconium are very small, since this insignificant amount has been distributed at a very small depth (near the surface of the film), its effects on surface properties, especially the number

of carriers and surface conductivity are very great.

3.5 Effects of doping on the detectors' properties

As mentioned, the main purpose of this study is to investigate the effect of sputtering of titanium and zirconium nanoparticles separately and both together on the properties of detectors. Accordingly, all the fabricated detectors were named and before doping, their transient response (in the form of an I-t test) was examined by placing them under a periodic UV illumination. After recording the relevant data, the I-t curve was plotted for each detector and by the use of it the main parameters of each detector was calculated according to the following definitions: 1. The maximum current under UV illumination (I_i) and the dark current (I_d), 2. photoresponsivity, $R \equiv I_{ph}/P_{op}$, where $I_{ph} = I_i - I_d$ is the photocurrent and P_{op} is the incident optical power, 3. rise time, RT, the time for the photocurrent to rise up from 10% to 90% of the peak value, and 4. fall time, FT, the time for the photocurrent to decay from the maximum to $1/e$ of it.

By reason of doping the detectors after electrode placement through LCST with Ti and Zr separately and with both together, the dark current and especially the maximum current of these detectors sharply increased. In addition, all their principal characteristics including the photoresponsivity and the response times (RT and FT) were intensely affected. To achieve a more accurate analysis of the effect of dopants on the important characteristics of the detectors and to take into account the statistical fluctuations, first the curves related to I-t tests of pre-doping and post-doping were plotted. Then, each of the main parameters in question (responsivity, RT, and FT) was calculated separately for four similar detectors fabricated on each substrate. And finally, the effect of doping on each parameter for each sputtering time interval was analyzed based on the average of the changes established in the four detectors with similar conditions.To better figure out the subject, for instance, figures(6-8) show the I-t curves of one of the four detectors on each substrate after sputtering with different dopants in terms of the type of dopant and the sputtering time. Furthermore, along with the curves concerning each dopant, a I-t curve of pure ZnO detector has been also plotted. By reason of the enormous difference in current in some curves, a different scale (second axis) has been used.

The photoresponsivity is the first parameter that one can calculate from the above I-t curves. Figure (9) indicates changes of the average R vs the sputtering time for singly-doped and co-doped ZnO detector with Ti and Zr. As seen from Fig 9, with the introduction of dopants and its increase up to 180 s sputtering, R increases in all detectors.This phenomenon can be attributed to the replacement of Zr^{4+} and Ti^{4+} ions with Zn^{2+}, which increases the number of free electrons [21–27]. These extra electrons can increase the responsivity by participating in oxygen absorption and desorption. As the sputtering time increases to more than 180 s, R decreases. At first glance, this reduction of photoresponsivity seems to be due to the formation of an opaque layer of dopant atoms on the detector
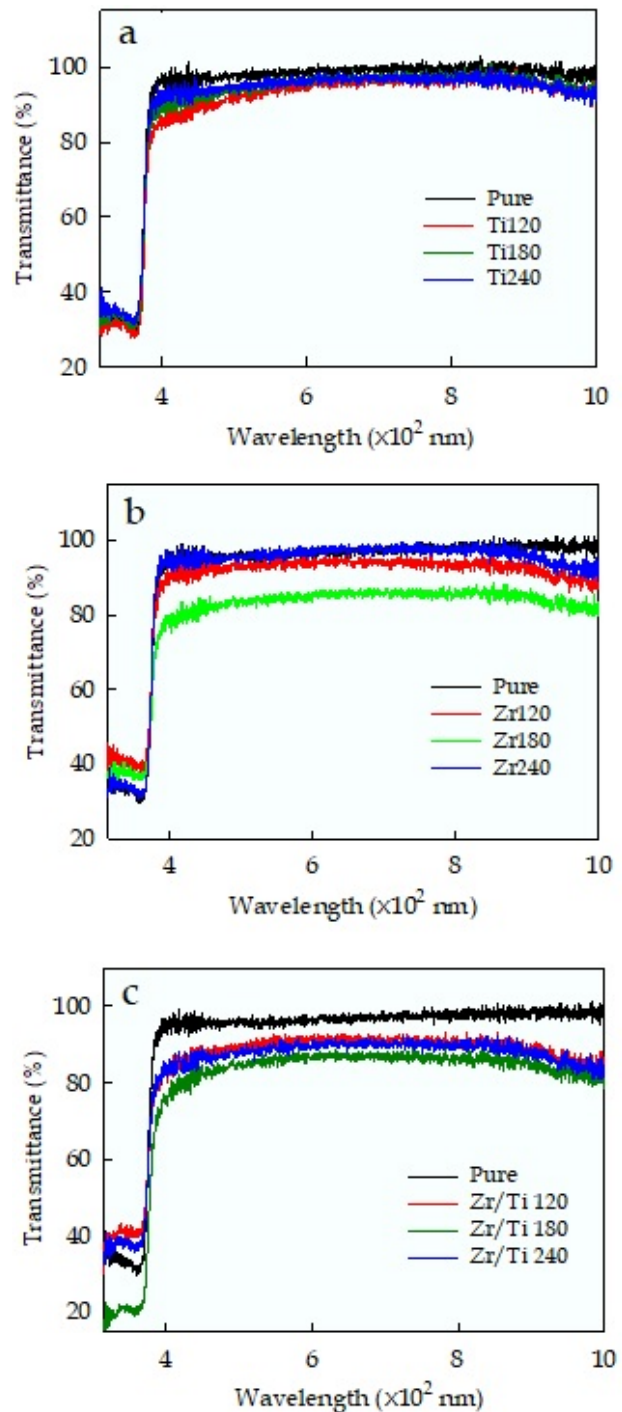
Figure 5. The transmittance of ZnO sensor doped with a) Ti, b) Zr, and c) both Ti and Zr along with the transmittance of a pure ZnO sensor

surface. But, it should be noted that since the sputtering operation is performed in a relatively short period of time and with a low current, a very small amount of the dopant introduces into the zinc oxide layer; the assertion that is also confirmed by the ICP-MS test. Therefore, the formation of such a layer does not appear reasonable. Moreover, the comparison of the

Table 1. The quantities measured related to pure and doped ZnO sensors, t_s: sputtering time; $\overline{RT}$: mean rise time; $\overline{FT}$: mean fall time; $\overline{R}$: mean photoresponsivity; $\overline{R}_{ad}$: $\overline{R}$ after doping; $\overline{R}_{bd}$: $\overline{R}$ before doping; Tr: transmittance.

Dopant	t_s (s)	$\overline{RT}$ (s)	$\overline{FT}$ (s)	$\overline{R}$ (A/W)	$\overline{R}_{ad}/\overline{R}_{bd}$	Tr (%)
Pure ZnO	0	20.3	0.6	0.068	-	97.0
Ti	120	25.5	1.2	0.42	~6	94.3
Ti	180	17.3	2.7	1.58	~23	95.5
Ti	240	12.5	1.0	0.51	~7.5	95.6
Zr	120	29.3	1.1	0.11	~1.5	92.2
Zr	180	>18.7	>10.7	29.17	>429	83.6
Zr	240	15.9	1.3	0.68	~10	95.6
Ti/Zr	120	9.9	0.7	0.54	~8	88.6
Ti/Zr	180	>24.7	>13.6	13.87	>200	83.8
Ti/Zr	240	14.7	1.6	2.33	~34	87.6

transmission spectra completely rejects the hypothesis of the formation of such an opaque layer. Because in none of the cases, the films that have the most doping do not have the lowest transmission coefficient.

Therefore, the decrease in R can be by reason of increasing the scattering phenomenon due to the presence of ionized dopants and also the segregation of Zr and Ti on the surface (whether in the form of neutral atoms [18] or their oxides [27]), which this occurrence, in turn, reduces the mobility of carriers and increases the electrical resistance. Similar phenomena have been reported in previous studies [23, 26, 27]. The im-

portant point to be noted here is that due to the fact that in co-doping of ZnO, more dopants introduce into the layer, it is expected that the steepest upward and downward slopes of R is related to the detector with co-doping process. But in practice, as can be seen from Fig. 9, this does not happen. This suggests the existence of another possible contributing factor, such as the mutual effect of Zr^{4+} and Ti^{4+} ions on the ZnO structure, which could be the subject of an independent study.

Another key characteristic of a detector that can be extracted through I-t tests is its response time, which is mostly mani-
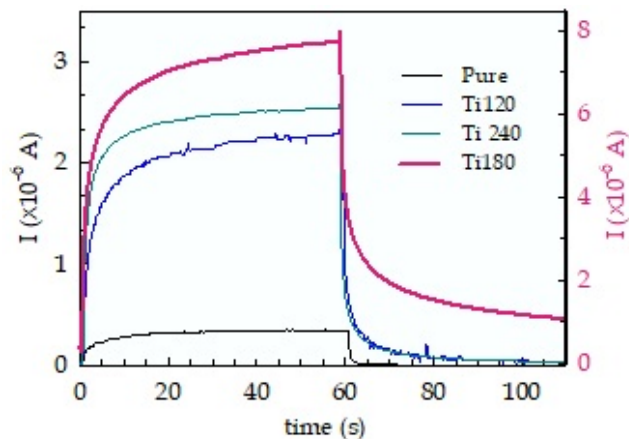
Figure 6. The transient response of the Ti-doped ZnO sensor along with that of a pure ZnO sensor obtained from I-t test
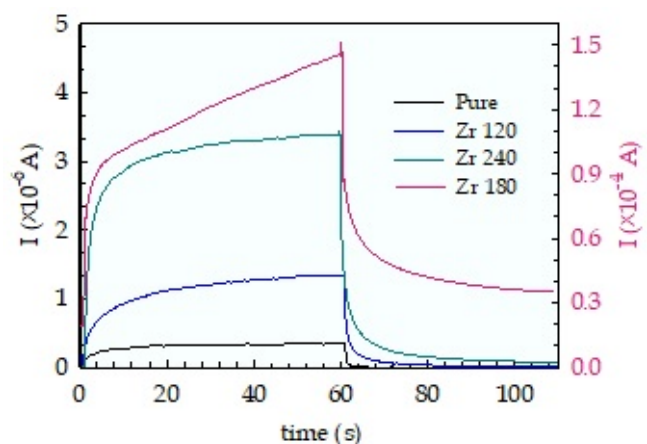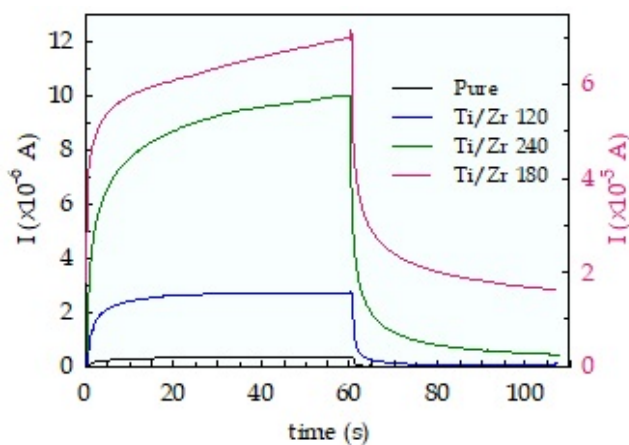

Figure 7. The transient response of the Zr-doped ZnO sensor along with that of a pure ZnO sensor obtained from I-t test

Table 2. Comparison between different results related to some other photodetectors with the one fabricated in this research, RT: rise time; FT: fall time; R: photoresponsivity; R_{ad}: R after doping; R_{bd}: R before doping; $N.C.$: no change; ↑: an increase in RT or FT; ↓: a decrease in RT or FT; Ag*: Ag nanoparticle [28–35].

nanostructure	dopant	R_{ad}/R_{bd}	RT changes	FT changes	reference
Thin Film	Al	1.54	< 3% ↓	-	[28]
Thin Film	Al	2.3	↑	↑	[16]
Thin Film	Ga	3.85	↑	↑	[16]
Microwire	Sn	~100	↑	↑	[29]
Thin Film	Dy	~31	~0.03% ↓	↑	[30]
Nanorod	Eu	<7	-	-	[31]
Nanorod	Fe	~7	-	-	[32]
Thin Film	Ag*	~100	-	-	[33]
Thin Film	Ag*	1.32	N.C.	N.C.	[34]
Nanorod	Cr	~3	-	-	[35]
Thin Film	Zr	5.3	~30% ↓	~33% ↓	[11]
Thin Film	Ti	>23	~15% ↓	↑	this work
Thin Film	Zr	>429	↑	↑	this work
Thin Film	Ti/Zr	~8	> 51% ↓	~N.C.	this work

fested in the form of two parameters: rise time and fall time. These two parameters for all the detectors were calculated before and after receiving the dopants, and the effect of the type of dopant and the sputtering period of time were investigated on their values. The results of the effect of doping in this method on the average values of RT, FT, and R parameters as well as the transmittance of all detectors are compared in Table 1. In Table 1, the declared values for each parameter have been determined from the average value of that parameter for the four identical detectors on a substrate associated with each process. An important conclusion to be drawn from the above results is that by singly and co-sputtering of Ti and Zr, R, RT, and FT can be managed. Comparison of test results, before and after doping, shows that not only have the photoresponsivity of all doped sensors improved, but some of these sensors have also concurrently experienced a significant decrease in rise time. The maximum increase in photoresponsivity is ob-

Figure 8. The transient response of the ZnO sensor co-doped with Ti and Zr along with that of a pure ZnO sensor obtained from I-t test
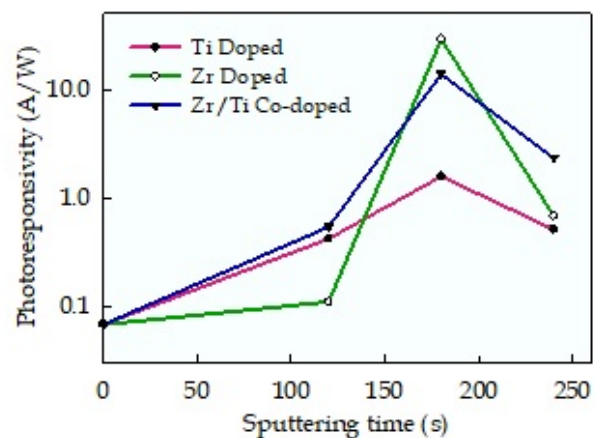
Figure 9. Changes of the photoresponsivity vs. sputtering time period for ZnO doped with Ti, Zr, and both together

served in sensors that have been sputtered for 180 seconds, which is more than 429, 200, and 23 times for doping with Zr, Ti+Zr, and Ti, respectively. In addition, the sensors which were co-doped with Zr and Ti for 120 s sputtering also show the greatest reduction in rise time to some extent more than 50% and simultaneously 8 times increase in photoresponsivity, this is while their fall time increase insignificantly.

Table 2 shows a comparison between the results of this study and other similar studies conducted to improve the performance of UV sensors through doping. Various factors such as the type of nanostructures, fabrication methods, the bias voltage, the intensity of radiation beam, and the shape and dimensions of the electrodes make the range of numbers reported for photoresponsivity and response time of ZnO-based sensors so different that it is difficult to compare them numerically. Therefore, instead of comparing the values of these quantities, comparing the changes of each quantity due to doping has been considered as a much more reliable parameter. Examination of the results of Table 2 indicates that doping with zirconium by the way carried out in this research establishes a high ability to control the properties of the sensor, especially the increase of photocurrent. The enhancement of dark and photo current owing Zr doping to an optimal extent, the conversion of ZnO layer to a transparent conducting oxide layer is also feasible [26]. On the other hand, the co-sputtering with titanium and zirconium shows the ability to significantly modify the photoresponsivity and the response time concurrently which is a great advantage, and circumstances like that has rarely been reported so far. Comparing the results of this research and the previous work [11], it can be concluded that, in addition to the type of nanoparticles, conditions of performing sputtering, especially its current, are also among the main parameters in how the projected nanoparticles affect the surface of sensors. Thus, by controlling the current, to a large extent, it is possible to change the method of introducing ions into the zinc oxide lattice in a controlled way and in addition adjust the properties of the sensor.

4. Conclusion

In this research work, the modification and adjustment of the properties of prefabricated ZnO-based UV sensors was performed by singly- and co-doping with zirconium and titanium nanoparticles through LCST. First of all, zinc oxide thin films were prepared by sol-gel method through spin coating and then converted to UV sensors by creating copper electrodes using the thermal evaporation method in vacuum and subjected to I−t test. In the next step, these sensors, each one including four similar detectors, were divided into three groups of three. The three sensors of the first group were doped with titanium through sputtering at time intervals of 120, 180 and 240 s, respectively. The sensors of the second group were also doped with zirconium in the same time conditions of the first group. While, the sensors of the third group were co-doped with Ti and Zr by participating in both processes of the groups 1 and 2. After doping, all sensors were again subjected to

I-t test. The results indicate that the photoresponsivity of all doped sensors has improved. Furthermore, some of sensors after doping have also concurrently experience a significant decrease in rise time. The maximum increase in photoresponsivity is related to sensors that have been sputtered for 180 seconds, which is more than 429, 200, and 23 times for doping with Zr, Ti+Zr, and Ti, respectively. In addition, the sensors which were co-doped with Zr and Ti for 120 s sputtering show not only the greatest reduction in rise time to some extent more than 50% but also a 8 times the photoresponsivity, while their fall time increases insignificantly. FE-SEM images, UV-visible spectroscopy, and XRD analysis indicated that despite very serious effects of this method on changing and adjusting the photoresponsivity and the response time, structural properties of the sensors such as the surface morphology, the crystalline structure, and the visible transmission coefficient do not change significantly due to doping. Overall, the results show that in this method, there is the ability to modify the desired features of a sensor in the shortest time and at the lowest cost for the intended purposes and to a large extent selectively. To modify and adjust many properties of UV sensors and even other sensors and actuators, it is obvious that singly- and co-doping of ZnO with a large number nanoparticles other than titanium and zirconium can be also performed using LCST, which it can be separately carried out in other researches.

Conflict of interest statement:
The authors declare that they have no conflict of interest.

References

[1] Ü. Özgür, D.Hofstetter, and H. Morkoc. *IEEE Conf. Proc.*, **1**:1255, 2010.

[2] S. G. Leonardi. *Chemosensors*, **5**:17, 2017.

[3] M. Laurenti and V. Cauda. *Coatings*, **8**:67, 2018.

[4] M. Laurenti and V. Cauda. *Nanomaterials*, **7**:374, 2017.

[5] R. Nisha, K.N. Madhusoodanan, T.V. Vimalkumar, and K.P. Vijayakumar. *Bull. Mater. Sci.*, **38**:583, (2015).

[6] G. Kumar R. Kumar, O. Al-Dossary and A. Umar. *Nanomicro Lett.*, **7**:97, 2015.

[7] S. Jeon D. Kim, W. Kim and K. Yong. *Nanomicro Lett.*, **7**:40539, 2017.

[8] H.M. Mahesh N. Srinatha, P. Raghu and B. Angadi. *J. Alloys Compd.*, **722**:888, 2017.

[9] A. Dugaya J. Chauhan, N. Shrivastav and D. Pandey. *J. Nanomed. Nanotechnol.*, **8**:1000429, 2017.

[10] C.S. Naveen H.M. Mahesh P. Raghu, N. Srinatha and B. Angadi. *J. Alloys Compd.*, **694**:68, 2017.

[11] E.A .Soleimani N. Madani Mashaei and H. Shirvani Mahdavi. *Appl. Phys. A*, **127**:204, 2021.

[12] Z. Khusaimi N.A. Abdullah and M. Rusop. *Appl. Phys. A*, **667**:329, 2013.

[13] Z.L. Wang. *J. Phys. Condens. Matter*, **16**:829, 2004.

[14] A.D. Trolio A. Guarino A.M. Cucolo A. Vecchione D. D'Agostino, C.D. Giorgio and F. Bobba. *J. Alloys Compd.*, **7**:055010, 2017.

[15] L. El Mir A. Bonavita N. Donato S.G. Leonardi M. Hjiri, R. Dhahri and G. Neri. *IEEE Conf. Proc.*, **634**:187, 2015.

[16] C.-Y. Tsay and W.-T. Hsu. *Materials*, **10**:1379, 2017.

[17] A.I. Mardare C. Kleber S. Huber, C.C. Mardare and A.W. Hassel. *RSC Adv.*, **9**:35579, 2019.

[18] C.-Y. Tsay and K.-S. Fan. *Mater. Trans.*, **49**:1900, 2008.

[19] L.-W. Ji I-T. Tang Y.-L. Chu, S.-J. Young and T.-T. *Chu, Sensors*, **20**:3861, 2020.

[20] S.H. Lee K.Y. Kang P.S. Shewale, N.K. Lee and Y.S. Yu. *J. Alloys Compd.*, **624**:251, 2015.

[21] X. Xian-Wu D. Ying L. Mao-Shui, P. Zhi-Yong and H. Sheng-Hao. *Chin. Phys. Soc.*, **16**:548, 2007.

[22] Z. Pang Y. Dai-L. Ye C. Cheng M. Lv, X. Xiu and S. Han. *Thin Solid Films.*, **516**:2017, 2008.

[23] S.K. Sen G.K. Paul, S. Bandyopadhyay and S. Sen. *Mater. Chem. Phys.*, **79**:71, 2003.

[24] M.M.M. Bilek D.R. McKenzie X.M. Duan, C. Stampfl and S.-H. Wei. *Phys. Rev. B*, **83**:085202, 2011.

[25] L. Hanfa Z. Huafu, L. Chengxin and Y. Changkun. *J. Semicond.*, **30**:043004, 2009.

[26] K. Durose G.J. Tatlock S. Herodotou, R.E. Treharne and R.J. Potter. *Materials*, **8**:7230, 2015.

[27] Y. Geng-Y.-Z. Gu Z.-Y. Xie Y. Zhang Q.-Q. Sun S.-J. Ding Z.-Y. Ye, H.-L. Lu and D.W. Zhang. *Nanoscale Res. Lett.*, **8**:108, 2013.

[28] A. Kumar D.K. Jarwal-R.K. Upadhyay A.P. Singh C. Kumar, B.K. Kushwaha and IEEE Photon S. Jit. *IEEE Photon. Technol. Lett.*, **32**:337, 2020.

[29] S. Wang L. Zhao X. Sun, F. Azad and S. Su. *J. Mater. Sci. Mater.*, **30**:518, 2019.

[30] R. Singh P. Kumar and P.C. Pandey. *J. Appl. Phys.*, **123**:054502, 2018.

[31] R. Azimirad M. Babamoradi, H. Sadeghi and S. Safa. *Optik.*, **167**:88, 2018.

[32] S. Safa R. Azimirad, A. Khayatian and M.A. Kashi. *J. Alloys Compd.*, **615**:227, 2014.

[33] J. Zhang G. Li, J. Song and X. Hou. *Solid State Electron*, **92**:47, 2014.

[34] X. Chen B. Li-M. Jiang Z. Zhang-H. Zhao X. Wang, K. Liu and D. Shen. *ACS Appl. Mater. Interfaces*, **9**:5574, 2017.

[35] A. Khayatian S. Mokhtari, S. Safa and R. Azimirad. *J. Electron. Mater.*, **46**:4250, 2017.